Mapping JWST Black Hole Data To Predicted Optimal Growth Conditions

Aidan Doyle
Conor Van Duyvenvoorde

Theoretical Physics department, Maynooth University

May 14, 2024

Abstract

New 2023 findings from the James Webb Space Telescope (JWST) suggest the existence of Supermassive Black Holes (SMBH) with mass in the range of 10^6 to 10^8, that are in place by $z \sim 10$, roughly 0.5 gigayears after the big bang. As it is incredibly difficult to reach such high masses in such a small time period, this implies a very high accretion efficiency within the standard Black Hole accretion models. Here we recreate statistical models, where we explore the conditions that lead to optimal growth for which Super Eddington accretion is permitted. Our analysis then allows us to map new SMBH findings from the JWST to these statistical models, providing insight into the initial conditions necessary for such high masses at such early stages in the universe. Analysis has suggested that the critical parameters from optimal growth in a SMBH are the initial black hole mass seed and the host galaxy central gas density. Super-Eddington accretion, for which the mass accretion rate exceeds the Eddington limit but the luminosity does not, is very effective in feeding a black hole. Even a short phase of super-Eddington accretion eases the time constraints. Through analytic calculations performed we find that the likelihood of such super-Eddington accretion becomes significantly more likely with an initial Black Hole seed mass $M_\bullet > 10^5 M_\odot$. Finalizing the results, we found there were holes in our understanding and possible improvements to the simulation. Further meticulous research is necessary if we want data that matches with real-world investigations.

1 Introduction

Since being launched in late 2021, the James Webb Space Telescope has provided new data which continually challenges our understanding of the cosmos. Supermassive black holes (SMBHs) with a redshift $z \sim 10$ ([1], [2], [3] and [4]) have been observed with estimated masses that lie on the very edge of what is possible at such an early time in the universe. To look at the possibility of reaching $M_\bullet \sim 10^8 M_\odot$ by such an early period in the universe, we need to take into account the initial masses and at what point in the cosmological timeline these black holes formed. The three types of stars leading to black hole formation are as follows.

- Population I stars: These stars form the most recent black holes in the universe and are highly metallic. Our Sun would be considered a population I star.
- Population II stars: Black holes formed by pop II stars are older black holes and would have been formed by a star with a low metal content.
- Population III stars: If a black hole was formed by a pop III star it was formed by one of the very first stars in the universe. These stars have next to no metal content. Theoretically it is expected that Pop-III stars are much more massive than Pop-II or Pop-I stars.

The problem becomes clear when we take an initial black hole mass relevant for all three populations and attempt to use standard models for black hole growth to recreate the SMBHs mentioned before. The standard formula for black hole mass growth ([5]) is in the form of an exponential function with a timescale $t_S \sim 0.045\epsilon_{0.1}$GYR, with $\epsilon_{0.1}$, the matter-radiation conversion factor normalized to a standard

value of 10%.

$$M_\bullet(t) = M_{\bullet,0} exp\left(\frac{t}{t_S}\right) \tag{1}$$

If we apply an initial black hole mass $M_\bullet < 100 M_\odot$, it becomes increasingly unlikely that a black hole will reach the predicted mass by a redshift of $z \sim 10$. Hence we are in need of a larger initial mass function for our black holes.
In ([6]) it is predicted that the first generation of very low metal cosmic structures formed massive stars, and thus allowed for higher mass black hole formations in the early universe. Another possibility is the predicted existence of Direct Collapse Black Holes (DCBH) ([7])). Self-gravitating gas in dark matter haloes can lose angular momentum rapidly. This leads to the rapid build-up of a dense, self-gravitating core supported by gas pressure – surrounded by a radiation pressure-dominated envelope – which gradually contracts and is compressed further by subsequent infall. This leads to high temperatures in the central region that the gas cools swiftly, leading to the formation and rapid growth of a central black hole. These black holes are predicted to have initial seed sizes of up to 10^5 solar masses.
These larger initial seeds will allow us to predict the possible growth for a Black hole mass seed, and give us a reference of what we should expect to see from recent JWST black holes.

2 Efficiency of Black Hole Growth at Different Scales

There are many factors that influence optimal conditions for black hole growth. As stated in ([5]), the most important physical effects that contribute are the radiation pressure and angular momentum of the black hole. When the combined effect of these two physical forces is ineffective at halting the accretion flow, we get optimal growth. This requires a smooth accretion flow at both large and small cosmological scales, however the set of conditions for these requirements differ drastically. The analysis conducted in ([5]) regarding the coupling between the black hole seed and its host halo was investigated in two-dimensional parameter space. The two parameters in this case being the initial seed mass $M_\bullet$, and the gas number density n_∞ of the host halo at the bondi radius defined to be $R_B = 2GM_\bullet/c_s^2$, where c_s is the speed of sound in the surrounding medium ([8]).

We will look at three conditions for optimal growth of a black hole seed in this parameter space, those being: growth efficiency with regards on small scales and on large scales, and with regards to angular momentum. In ([5]), the host galaxy has an isothermal density profile for the gas it contains:

$$\rho(r) = \frac{f_g \sigma^2}{2\pi G r^2} \tag{2}$$

where $f_g = \Omega_b/\Omega_m = 0.16$ is the cosmological gas fraction and the velocity dispersion σ is linked to the halo mass, following ([5]).
To understand the growth efficiency of black holes we need to understand the transition radius R_t ([9]). Described as the spatial scale above which the accretion flow is dominated by radiation pressure that powers outflows, the transition radius is the radius r at which the feedback t_{fb} and the accretion t_{acc} times equal. In this case the feedback timescale is defined as the time needed by radiation pressure to significantly change $\dot{M}_\bullet$, the rate of change of the black hole mass, and the accretion time-scale which estimates the time needed to consume the gas mass inside the inner regions of the accretion flow.
Another important part for understanding growth efficiency is the photon trapping radius ([10]). Given as:

$$r_{tr} = \frac{\dot{M}}{\dot{M}_E}\frac{r_s}{2} \tag{3}$$

where r_s is the Schwarzschild radius and $\dot{M}_E \equiv L_E/c^2$ with L_E denoting the Eddington limit.
It is defined by "setting the infall speed of the gas $v(r_{tr})$ equal to the approximate outward diffusion speed of the radiation $c/\tau(r_{tr})$, where $\tau(r) \equiv \rho(r)\sigma_T r/m_p$ is the optical depth along a column of gas spanning distance r at density $\rho(r)$." In more simpler terms the distance from a compact object (like a black hole) where photons (particles of light) are no longer able to escape freely due to the strong gravitational pull of the object. This radius marks the point at which photons become trapped and cannot escape, being pulled into the object.

2.1 Growth Efficiency on Small Scales ($r \ll R_B$)

The growth efficiency on small scales is based on the transition radius as defined previously. We know that at the transition radius: $t_{fb}(R_t) = t_{acc}(R_t)$
As noted in ([11]) and ([9]) R_t then splits apart the two accretion regions. Firstly a"gas-supply limited" regime in which the flow is "feeding-dominated" where $r \ll R_t(t_{acc} \ll t_{fb})$ and gas is accreted efficiently. The other regime has a "feedback-limited" flow in which $r \gg R_t(t_{acc} \gg t_{fb})$ and the accretion proceeds in an intermittent way or can even stop completely with an empty gas reservoir. In ([5]), the transition radius is compared to another typical spatial scale, Photon trapping ([10]) to allow for additional forces other than gravity and radiation pressure to have an effect. This comparison gives rise to the following small scale condition:

$$M_\bullet > 10^{-11} \left(\frac{n_\infty}{1cm^{-3}}\right)^2 M_\odot \tag{4}$$

To sustain optimal growth, this equation suggests that an increase in the gas number density of the host galaxy would need to be met with an adequate increase in the minimum seed mass of the black hole. A larger n_∞ potentially leads to a larger accretion rate, however this would suggest that to sustain this larger accretion rate you need a large enough initial black hole.

2.2 Growth Efficiency on Large Scales ($r \geq R_B$)

The efficiency of black hole growth on large spacial scales was examined in ([12]). To induce a steady accretion that is hyper-eddington and overcomes radiative feedback we have the following condition:

$$\left(\frac{n}{10^5 cm^{-3}}\right) > \left(\frac{M_\bullet}{10^4 M_\odot}\right)^{-1} \left(\frac{T}{10^4 K}\right)^{3/2} \tag{5}$$

In such a hyper-Eddington scenario, the solution comprises of two main parts: a central core, which is the region in the system where most of the radiation is concentrated and where the trapping of photons due to electron scattering is significant, and an outer layer that's accreting material along a Bondi profile. Because photon trapping has a significant effect, the radiation emitted from the core doesn't significantly change how gas behaves on larger scales, allowing super-Eddington accretion rates to continue. If we let $T \sim 10^4 K$, meaning that the gas is at the atomic cooling threshold, we can change this equation to a relation between M_{BH} and n_∞:

$$M_\bullet > 10^9 \left(\frac{n_\infty}{1cm^{-3}}\right)^{-1} M_\odot \tag{6}$$

This inequatlity would suggest that an increase in n_∞ would lead to a decrease in the necessary minimum seed mass of the black hole. In fact, when there's more gas around, it can lead to higher rates of material being pulled in, which makes photon trapping more important. This means the H-II region (ionized gas region) around the black hole stays smaller than the Bondi radius, allowing large amounts of gas to move from bigger to smaller areas more easily. Note that the assumption that the gas is at the atomic cooling threshold is only possible in the early (high redshift) universe.

2.3 Growth Efficiency and Angular Momentum

Gas with Keplerian angular momentum cannot reach the black hole via free-fall from any radius $R > R_s$. However, when the rotation is sub-Keplerian the gas can fall into the black hole even from $R > 3R_s$ ([13]). Thus we know that there is a significant angular momentum barrier that infalling gas needs to overcome before it can accrete effectively. ([5]) references a 2017 paper ([14]) that investigated how infalling gas must have a sufficiently low angular momentum in order for it to be accreted at a "hyper-Eddington" rate.

A dimensionless angular momentum parameter λ_b is defined as $\lambda_b = l_b/(GMR_s)^{1/2}$ where l_b is taken to be the specific angular momentum of the gas at the accretion radius. There are several regimes within the accretion process which change depending on l_b, however for the most optimal accretion:

$$\lambda_{b,crit} = 0.1\sigma_{100}^{5/2} \left(\frac{\dot{M}}{\dot{M}_{ff}}\right)^{1/2} \left(\frac{M_\bullet}{10^6 M_\odot}\right)^{-1/2} \tag{7}$$

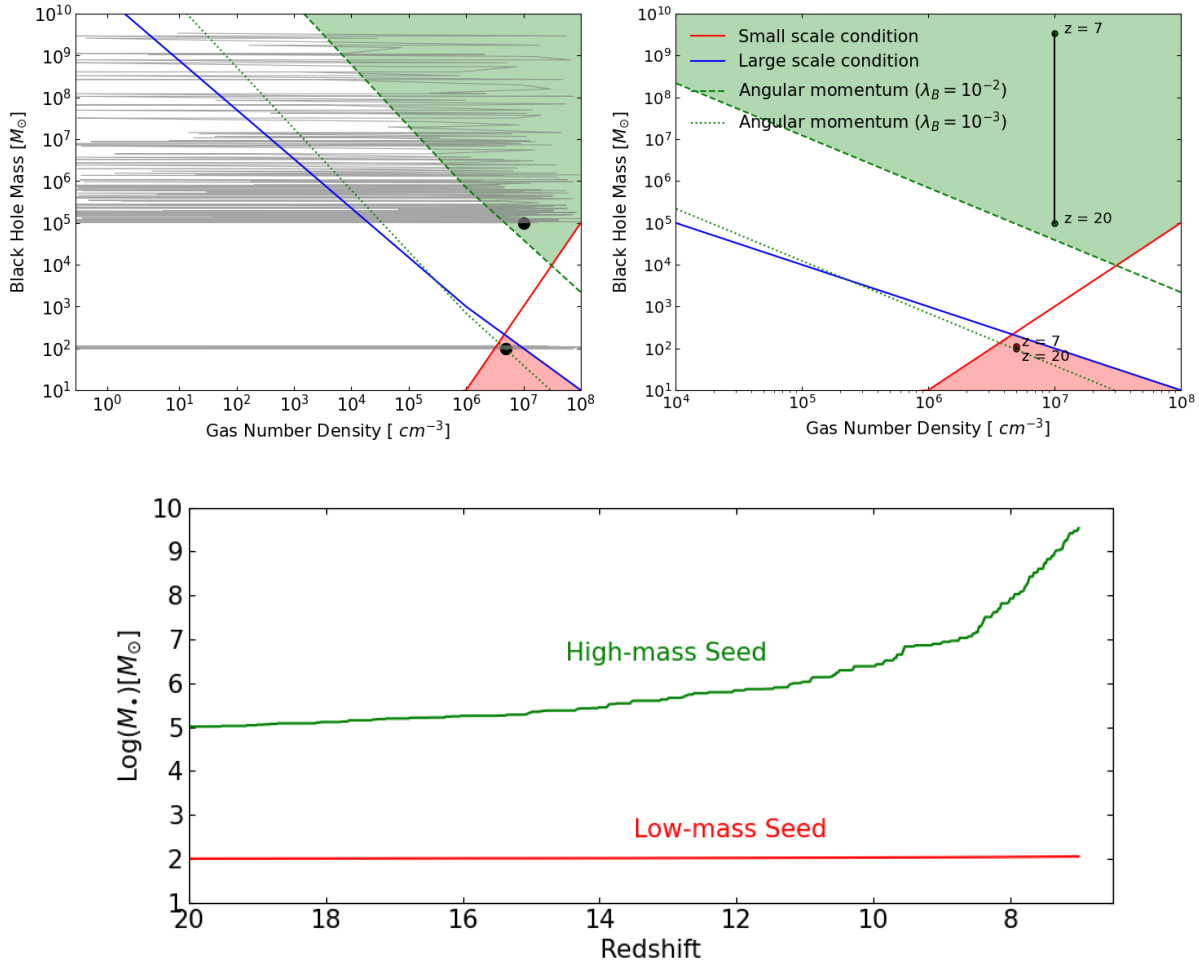

Figure 1a: (left) Showing the relationship between the small scale (red line), large scale (blue line), and angular momentum (green dashed lines) conditions in the $M_\bullet - n_\infty$ parameter space. The green shaded region represents the efficient region in which all three conditions are met and accretion rates are high. The remaining space is considered inefficient especially the red region where none of the conditions are met, we call this the 'super bad' region. Almost no accretion occurs here. We have also graphed the cosmological evolution of two black holes (initial conditions represented by black circles) from $z_0 = 20$ to z = 7. Black hole 1 starts off in the efficient region with initial mass $M_{\bullet,1} = 10^5 M_\odot$ and initial gas number density $n_{\infty,1} = 5$ x $10^6 cm^{-3}$. While Black Hole 2 starts in the 'super bad' region with initial mass and gas number density $M_{\bullet,2} = 10^2 M_\odot$, $n_{\infty,2} = 5$ x $10^7 cm^{-3}$ respectively. The grey lines represent each black hole's growth. At each time step we take a uniformly random gas number density between $10^{-2} cm^{-3}$ and $10^8 cm^{-3}$ and evolve the black hole in accordance with its instantaneous position in the space. We can see that the larger seed easily reaches $10^9 M_\odot$ by z ~7.

Figure 1b: (Right) This shows the evolution of the seeds in the 2 parameter space more clearly. Keeping the density constant to make it easier to interpret we can see the start and end points of each black hole's growth (green circles for BH1 and red circles for BH2). We also have two different Angular momentum conditions, one using $\lambda_b = 10^{-2}$ which corresponds to the dashed green line and the other using $\lambda_b = 10^{-3}$ corresponding to the dotted green line.

Figure 1c: (Bottom) Illustrates the evolution of the black holes with respect to redshift. The High-mass (Low-mass) black hole is shown by a green (red) line.

The critical value of λ_b suggests that the gas hits a point where centrifugal forces counteract gravity after passing through the trapping radius. This implies that angular momentum builds up when the gas is highly trapped, resulting in ineffective repulsion by radiative pressure. This setup feeds the black hole at an extremely high rate. (The lower limit implies that the gas has too much angular momentum and must dissipate some energy, however this is expected to be satisfied in almost all cases). We can reorganize this condition in terms of n_∞ and $M_\bullet$, where λ_b is a free parameter, giving us:

$$M_\bullet > 2.2 \times 10^{19} \left(\frac{n_\infty}{1cm^{-3}}\right)^{-5/4} \lambda_b^3 M_\odot \tag{8}$$

2.4 Conditions for the Optimal Growth of Seeds

If we look at the righthand graph in Figure 1, it shows the relation between the large and small scale conditions, along with the angular momentum conditions in the $M_\bullet - n_\infty$ parameter space. Note that for a black hole to be considered to highly efficient, it must satisfy all three conditions in equations (4), (6), (8).

Denoted by the green section in Figure 1, the high efficiency region is the region where all three conditions are met. If a black hole seed finds itself in this region it is considered an "efficient accretor" as its combination of $M_\bullet$ and n_∞ allows it to absorb a steady stream of gas unimpeded, contributing to significant growth. Accretion outside this zone, where one of the conditions is not met, is called a "Low Efficiency Accretion region". These zones are indicative with either a low duty cycle or low accretion rates, possibly both. On the graph we also note a zone where all three conditions are not met. In this zone a black holes accretion rate is negligible and it will struggle to grow. The region a black hole forms in quite often determines its ability to grow, with larger black holes commonly forming in the high efficiency region while ones that form outside this region will usually stay small. We will later look into the probability of a black hole forming in each respective section. (Section 4)

3 Cosmological Evolution of Seeds

Continuing on from defining the conditions for optimal black hole growth, we also want to be able to predict the evolution of growth of an initial black hole mass seed over time. Following the work done in ([5]), the time evolution of the black hole mass is described using two parameters, those being: (i) the Duty cycle $\mathcal{D}$. Where $\mathcal{D} \equiv 1 - t_{idle}/t_{tot}$ is the fraction of time spent accreting. (ii) the Eddington ratio $f_{Edd} = \dot{M}/\dot{M}_{Edd}$. In this case, the duty cycle will describe the continuity of mass inflow while the eddington ratio will tell us the amount of mass flowing in.
We can then parameterize the time evolution of $M_\bullet$ as follows:

$$\frac{dM_\bullet}{dt} = \mathcal{D} f_{Edd} \dot{M}_{Edd} = \mathcal{D} f_{Edd} \frac{4\pi G}{c\kappa_T} M_\bullet \tag{9}$$

We wish to get this equation in terms of redshift. This derivation was taken to be trivial in ([5]), however it is very much not. We can express the desired equation in the following form:

$$\frac{dM_\bullet}{dz} = \frac{dM_\bullet}{dt}\frac{dt}{dz}$$

The universe in this case is presumed to be radiation-less and curvature less. Now starting with the friedmann equation, we will derive a formula for dt/dz:

$$\left(\frac{1}{a}\frac{da}{dt}\right)^2 = H_0^2(\Omega_m a^{-3} + \Omega_\Lambda)$$
$$\left(\frac{da}{dt}\right)^2 = a^2 H_0^2(\Omega_m a^{-3} + \Omega_\Lambda)$$

We know $\Omega_M + \Omega_\Lambda = 1$. Using this we can get:

$$\left(\frac{da}{dt}\right)^2 = H_0^2(\Omega_m a^{-1} + \Omega_\Lambda a^2 + 1 - \Omega_m - \Omega_\Lambda)$$
$$= H_0^2(\Omega_m(a^{-1} - 1) + \Omega_\Lambda(a^2 - 1) + 1)$$

and hence

$$\frac{da}{dt} = \frac{da}{dz}\frac{dz}{dt} = H_0(\Omega_m(a^{-1} - 1) + \Omega_\Lambda(a^2 - 1) + 1)^{1/2}$$

Using the fact that $a = \frac{1}{1+z}$, we find that $\frac{da}{dz} = \frac{-1}{(1+z)^2}$

$$\frac{da}{dz}\frac{dz}{dt} = \frac{-1}{(1+z)^2}\frac{dz}{dt} = H_0(\Omega_m(a^{-1} - 1) + \Omega_\Lambda(a^2 - 1) + 1)^{1/2}$$

giving us that

$$\frac{dt}{dz} = \frac{-1}{H_0(1+z)^2(\Omega_m(a^{-1} - 1) + \Omega_\Lambda(a^2 - 1) + 1)^{1/2}}$$
$$= \frac{-1}{H_0(1+z)\sqrt{(1+z)^2(\Omega_m + 1) - \Omega_\Lambda z(z+2)}}$$

Therefore

$$\frac{dM_\bullet}{dt} = -\frac{\mathcal{C}M_\bullet}{\mathcal{E}(z)}$$

Where we define

$$\mathcal{C}(\mathcal{D}, f_{Edd}) = \frac{4\pi\mathcal{D}f_{Edd}}{H_0 c\kappa_T}$$

and

$$\mathcal{E}(z) = (1+z)[(1+z)^2(\Omega_m + 1) - \Omega_\Lambda z(z+2)]^{1/2}$$

Although not separated in ([5]) we will separate the constants from the Duty cycle and the eddington ratio for simplicity. The local value of the Hubble constant will also be taken to be constant (~ 69) in this case. The values for $\mathcal{D}$ and f_{Edd} will be taken from ([9]), ([12]), and ([14]). In the high efficiency region, we will take $\mathcal{D} \sim 1$ and $f_{Edd} \gg 1$, and in the low efficiency region $\mathcal{D} \ll 1$ and $f_{Edd} \ll 1$.
To find how $M_\bullet$ changes with respect to redshift, we integrate, starting the evolution from redshift z_0 with a corresponding seed-mass $M_\bullet$ we obtain:

$$M_\bullet(z) = M_{\bullet,0} exp\left(\mathcal{C}\int_z^{z_0}\frac{dz}{\mathcal{E}(z)}\right) \tag{10}$$

In ([5]) it is also noted that the gas density around the black hole will vary with redshift due to a multitude of factors, including potential galaxy mergers and thermodynamic effects such as supernovae, and outflow. Finding an exact prediction of the gas density around a black hole at any redshift would be nye on impossible and thus we will make predictions based on previous works. As noted in ([12]), a gas number density range of $10^{-2} < n_\infty(cm^{-3}) < 10^8$ would adequately consider the diverse dynamics of halo histories and the baryonic characteristics during these cosmic epochs. We will draw random variables from this range, creating statistical outcomes which are idealistic in nature, but conservative enough to create an accurate prediction for black hole growth.

Visible in the left most panel in Figure 1, are two separate paths on the graph which represent the cosmological evolution of seeds. Starting at $z_0 = 20$ and continuing up until $z = 7$, they represent the two most extreme cases possible within our model, those being a black hole with incredibly high accretion efficiency and one which backs up the lower end on the efficiency scale. These two cases are also present in the right-hand panel of Figure 1, however in this case the growth is merely presented from start to finish, to better show the difference in total growth.

The initial mass density n_∞ was also set explicitly. Many other works (e.g: ([15]), ([16])) have shown previously that a low-mass seed is expected to form in a low density region, and similarly a high-mass seed is expected to have a large initial density ([9]). Following the work done in ([5]) The seeds are then evolved from $z = 20$ to $z = 7$, in 100 steps equally spaced in redshift. At each step, the new density is drawn from a uniform distribution in the range $-2 < Log_{10}(n_\infty[cm^{-3}]) < 8$, while the mass is evolved according to our integral equation. F_{Edd} and $\mathcal{D}$ are the only two dependent variables present in our equations, and thus we must pick them according to which efficiency region the black hole seed is in. First looking at the high-efficiency region, these parameters are drawn from a uniform distribution with ranges $0.5 < \mathcal{D} \leq 1, 1 \leq f_{Edd} < 100$. For the low-efficiency region, looking again to a uniform distribution for the parameters, we take them within the ranges $0 \leq \mathcal{D} \leq 1, 0 \leq f_{Edd} < 1$.

In the third graph present in Figure 1, we present the linear growth of the black hole seeds throughout time, and will allow us to visually map more current data from black holes found by the JWST to these pedictions. In this case the green line representing the growth of the high-efficiency seed and the red line representing the growth (or lack thereof) of the low-efficiency seed.

4 Probabilistic view of growth

In the previous sections we have inserted constraints, in line with conditions present in the high redshift universe, that have allowed us to create a probabilistic view of early black hole growth. Again following ([5]), we will now insert distributions, in line with expected initial masses of black holes in the early universe, to allow us to get a visual representation of the quantity of black holes that could form in the high efficiency region. The previous graphs in Figure 1 suggest that any black hole seed formed in the high efficiency region would likely grow very rapidly, and vice versa, any black hole formed outside of this region would likely be ineffective at accreting gas and thus would have a protracted cycle of growth. The likelihood that a black hole forms at any given initial mass is not equal, and are randomly distributed along an initial mass function (IMF). If we compare these initial mass functions with the high efficiency region in our two-parameter space, it will allow us to more accurately predict the likelihood that a seed reaches the SMBH stage rapidly.

The paper maps two kinds of early universe black hole formations, namely Direct Collapse Black Holes (DCBH) , and Pop-III remnants.
Modelling the initial mass function (IMF) of DCBH is notoriously difficult, thus we will reference results from ([17]). Taken from the "fertile model" section, we find the IMF valid for intermediate mass black holes (IMBHs) mapped with a Gaussian distribution:

$$\Phi(DCBH) = NORM(Log\mu = 5.1, Log\sigma = 0.2) \tag{11}$$

Where in this case μ is the mean and σ is the standard deviation. (mentions that bimodality of the guassian doesn't matter but why) For the pop III remnants, we use results from ([18]); ([19]), using a far simpler model with a decreasing exponent and includes a low mass cut-off M_c

$$\Phi(Pop - III, m) \propto m^{-2.35} exp\left(-\frac{M_c}{m}\right) \tag{12}$$

Where m is measured in solar masses. For Pop-III stars the low mass cut-off is taken to be $M_c = 10M_\odot$. Also taken into account from ([20]) is the gap formed by the pair instability supernovae ($100 - 160M_\odot$), which leave no remnant.
Following [5], the quantity $\mathcal{R} \equiv N_{DCBH}/N_{PopIII}$ is the ratio of the number of DCBH compared to the number of Pop III black holes, and is estimated using the luminosity function of high redshift quasars.

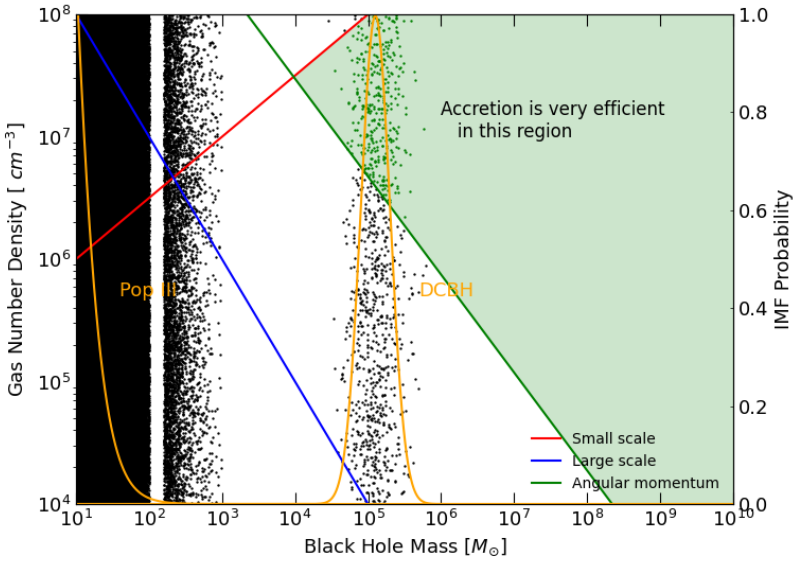

Figure 2: Showing the probability that a black hole seed is formed in the efficient region. The IMFs for the DCBH and Pop-III seeds are shown by orange lines (using the right axis labels). We used an Ensemble of 10^6 black holes with $\mathcal{R} = 10^{-3}$ (black dots). The ones in the high-efficiency region are green. We assume the gas number density is equally probable over the range $10^4 < n_\infty < 10^8$ while the black holes follow their respective IMFs. We get an average of 350 black hole seeds formed in the efficient region over multiple runs.

(e.g., Masters et al. 2012, which uses the COSMOS photometry) In our model we use $\mathcal{R} = 10^{-3}$ with a total ensemble of 10^6 black holes populating Figure. Assuming that the high-luminosity quasars are produced by high-mass seeds, and low-luminosity quasars by low-mass seeds, we generalise the results up to a redshift of $z \geq 7$.

5 Mapping JWST black holes to predicted growth

As referenced in the introduction, the JWST has found multiple SMBHs which seem to exceed the possible mass attainable at such high redshifts. The four SMBHs we will map to our data are:

- GN-Z11: $z \sim 10.6$ and $M_\bullet \sim 2 \times 10^6$ ([3])
- UHZ-1: $z \sim 10.1$ and $M_\bullet \sim 4 \times 10^7$ ([1])
- GHZ-9: $z \sim 10$ and $M_\bullet \sim 8 \times 10^7$ ([4])
- CEERS-1019: $z \sim 8.7$ and $M_\bullet \sim 9 \times 10^6$ ([2])

Using Figure 1c, which shows the predicted linear growth of a black hole seed with respect to redshift. We now plot the JWST SMBHs with respect to this graph to give a visual representation of their magnitude:

6 Observational results

First we will start with some observational consequences of we can deduce from Figure 1. Starting with black holes that start in the low efficiency region, which are characterized by their low eddington ratio (Fedd) and low duty cycle (fD). It is predicted in ([5]) that there exists a whole class of these low efficiency black holes which would be largely unobservable to us currently due to both their low luminosity, which is proportional their eddington ratio's, and also these black holes will be accreting for only a small fraction of time, due to their low duty cycles. Along with a selection of faint quasars in deep surveys, which are

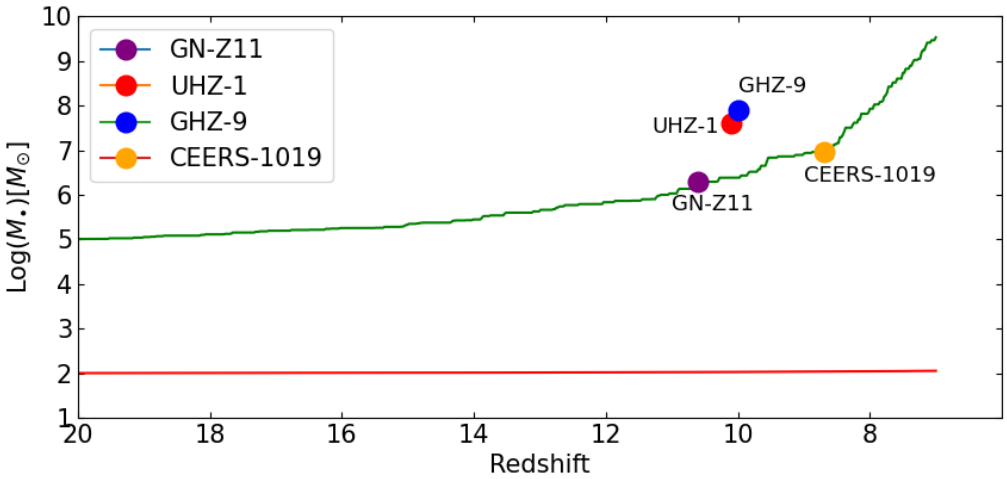

Figure 3: The graph shows the SMBHs plotted against the evolution simulation in Figure 1c. Two of which lie very close to what the optimal growth conditions predict we should have. Both CEERS-1019 and GNZ-11 match the predicted high efficiency growth scenario which would suggest that although unlikely, these SMBHs are more completely feasible. On the other hand we have two of the SMBHs which are placed alarmingly far above the line. GHZ-9 and UHZ-1 have masses which are not predicted until a redshift around $z \sim 7.5$, roughly 0.3 GYR's later. This poses a severe issue for our understanding of the formation of SMBHs.

predicted to be obscured by a large column densities in their host galaxies, (([21]); ([22])), there should exist another population of undetectable black holes. There does exist some evidence for these populations in studies ([23]);([24]), where there was detection of gravitational waves of their merging activities.

Conversely, we expect that at high-redshifts, high mass-seeds would proportionally be detected far more frequently than their corresponding low mass seeds. The presence of super-Eddington accretion, which benefits their already bright luminosity, would make them far easier to detect than the low luminosity black holes.

In Figure 2 you can see the initial mass functions of the pop III stars and the DCBH, mapped in relation to the high efficiency accretion region. It is quite clear that the pop III stars form at a far too low mass to start off as efficient accretors, and will form in the highly inefficient zone a large percentage of the time. The Direct collapse Black holes however are capable of being formed within the bounds of the high efficiency accretion region, and are thus better candidates for forming SMBH in the early universe.

Figure 3 shows that two of these SMBHs lie very close to what the optimal growth conditions predict we should have. Both CEERS-1019 and GNZ-11 match the predicted high efficiency growth scenario which would suggest that although unlikely, these SMBHs are more completely feasible. On the other hand we have two of the SMBHs which are placed alarmingly far above the line. GHZ-9 and UHZ-1 have masses which are not predicted until a redshift around $z \sim 7.5$, roughly 0.3 GYR's later. This poses a severe issue for our understanding of the formation of SMBHs.

7 Discussion and conclusion

It is clear from our predictions that to be able to reach such large black hole masses at such large redshifts as observed recently by JWST, a near constant accretion rate is required. In this paper we reproduced predictions made in ([5]), combining the factors required for small scale conditions, large scale conditions and bearing in mind the angular momentum of the infalling gas to create optimal growth conditions. We try to find a path for efficient accretion through the early universe, in a two parameter $M_\bullet - n_\infty$ space, showing the possibility of reasonably reaching a black hole mass of $10^9 M_\odot$ by a $z \sim 7$. We then mapped recent Black hole discoveries ([3], [1], [4], [2]) to this data to see if it matches the predictions made.

From Figure 1 it becomes evidently clear that there exists a region, for $M_\bullet \geq 10^5$, that suggests incredibly efficient accretion for any black hole seed within it. This implies a near continuous duty cycle ($\mathcal{D} \sim 1$) and a large accretion rate ($F_{edd} \gg 1$). Thus it is possible for a black hole seed which is constantly within this region to reach (and exceed) the observed black hole mass by such early redshifts. On the other hand however we also have a region we labelled the inefficient accretion zone. In this zone the black hole growth is negligible.

These two zones allow us to generate a uniformly random n_∞ at each time step such that $-2 < Log_{10}(n_\infty[cm^{-3}]) < 8$. This is done to simulate the possible change in the gas number density over time. We get out a prediction of the possible growth of the mass of a black hole seed, which grows efficiently when the random n_∞ places it in the high efficiency zone, and grown inefficiently otherwise.

Using this we create two separate models of growth, one for a low-mass seed, and one for a high-mass seed. Low-mass seeds form in low-density regions and high-mass seeds form in high density regions (([15]); ([16])). This allows us to set the initial densities for each model of growth.
Figure 2 then allows us to predict the probability that a given initial mass seed will start within the high accretion zone. We look at two possible types of black hole formation which could possibly lead to such high initial masses: DCBH and Pop-III black holes. Mapping the IMF of DCBH with a normal distribution ([17]) and of Pop-III black holes with a simplistic model (([18]), ([19])), it becomes evidently clear that the probability of an initial black hole seed falling within this zone is incredibly unlikely.

Note that the ratio of DCBH to Pop-III black holes ($\mathcal{R} = n_{DCBH}/n_{PopIII}$) is set to 10^{-3} for Figure 2 (([25]),([5])). Thus implying that a DCBH is rare in itself when compared to a regular Pop-III star. The Pop-III stars fall far below the required initial mass to be within the high efficiency zone, meaning that none of these could possibly become the required SMBH's so early in the universe. Thus we are relying solely on the DCBH's to form our required initial mass seeds.

Taking this at face value it would suggest that finding a Black hole seed with such high initial mass would be unlikely, although not impossible. This could be misleading however. It is predicted in ([26]) that initially high-mass $\sim 10^5 M_\odot$ seeds grow rapidly in number during a limited time period in the early universe, since DCBH formation leads to the emission of Lyman-Werner photons that seed the formation of other DCBH. This implies that in the early universe the difference in number of DCBH's to Pop-III black holes could be smaller, and thus making it more likely that a SMBH large enough would form over time.

Lastly in Figure 3 we plot four of the JWST black holes (([4]), ([1]), ([2]), ([3])) onto Figure 1c. In Figure 1c we show the predicted growth of both the high initial-mass and low initial-mass seeds plotted in solar masses against redshift. As discussed early in (section 6) it is clear that there are two black holes which lie significantly above where the predicted high-efficiency growth would expect them at the corresponding redshift. This seems to suggest that there is an issue with our understanding of black hole formation and accretion, however there are some caviats: (i) The gas number density is incredibly variant throughout time. A more stable gas number density could allow for a high initial-mass black hole to stay within the high efficiency accretion zone for far longer periods of time, and thus become larger than our model predicts. This is evident in our simulation through the change from run to run, where two consecutive timesteps in the high-efficiency region lead to a signifact increase in mass. (ii) This simulation relies only on initial mass and gas number density and does not allow for any of the smaller factors that can have a significant affect on the mass of a black hole (e.g: dynamical friction ([27]).

Overall, by assessing how the gas number density and angular momentum affect black hole accretion, we have been able to create optimal growth scenario's in the $M_\bullet - n_\infty$ parameter space. Then looking at the IMF for two main types of black hole formation, we are able to predict the likelihood of an initial black hole seed forming within the given high efficiency region. Using this information we then mapped the potential growth of given black hole seeds from a redshift $z = 20$ to redshift $z = 7$ which allowed us to visualize the new JWST SMBH data on this graph. We found that (as predicted) some of these SMBH's had an unexpectedly high mass at their respective redshifts. The data may not present an accurate picture however, with it only taking into account two parameters, and using randomized values for the gas number density at each time-step. This could lead to inaccuracies which prevent growth of each seed in our model. However if these fears are unjustified, and the size of these SMBH's cannot be explained,

then this presents a distinct challenge to our comprehension of the early universe and the formation of the first black holes.

Numerical methods and acknowledgements .
The Python code wasn't too difficult for this project but it did take some background knowledge to know what we were looking at. For Figure 1, we used matplotlib and a simple for loop to plot the conditions necessary for efficient growth. We found the fill-between command from matplotlib.pyplot only filled the left and right sections of the condition lines. So we filled everything above and below the lines with the required colour and then we filled the excess with white, and it solved the problem. For the grey lines in Figure 1 at each time step we drew a uniformly random gas number density between -2 and 8 and reversed the logarithm after so that there wouldn't be a big bias towards the higher densities. Given the mass and the gas number density at each time step we decided what $\mathcal{D}$ and F_{edd} we would use in the calculations. We then calculated the integral and evolved the mass according to (10). Plotting this against the gas number density gives the plot in Figure 1a. Plus the initial conditions plotted as big black dots.

For Figure 1b it is very similar but we changed the limits of the x-axis to 10^4 to 10^8 and we plotted the initial and final states of the 2 black holes only. Putting some text in accordingly for labels. All we did in Figure 1c was plot the masses of the black holes against the redshift, it doesn't look smooth as at each time step theres a random chance that it will end in the efficient region so it won't accrete the entire time.

For Figure 2 we first plotted the given DCBH and Pop-III distributions while finding their normalization constants. We plotted them with respect to the right axis to keep it consistent with the other figures. To plot all the black hole seeds we generated random numbers based on the distributions and used pyplot.scatter to plot them against a uniformly random gas number density as before. It was tough to do this for the custom distribution for the Pop-III distribution but we just turned it into it's cumulative distribution function using np.cumsum. After that we normalized it to values between 0 and 1, then interpolated it using np.interp to give our random masses. Plotting 10^6 total black holes, with $\mathcal{R} = 10^{-3}$. We couldn't find the IMF for the section after the gap corresponding to the pair instability supernovae so we just kept those in-line with the Pop-III distribution. We made the gap itself by splitting the array of masses into two sections, one from 1 - 2 and the other from log(160) - 3 and putting them back together, reversing the logarithms after to get the desired mass distribution.

Finally, for Figure 3, simply we plotted the JWST black holes against the plot in Figure 1c, using different colours to distinguish them.

We also had a bit of trouble with the constant $\mathcal{C}$ in (10). We tried to calculate it by hand making sure the units were correct but no matter how much we looked into the values of the given constants, it didn't result in the plots we were expecting. We found it was off of the expected value by a factor of $\sim 10^7$ so we decided to leave it as we were wasting too much time on it. We did all future calculations with an estimated value of 24 giving us a consistently satisfying plot.

We would like to thank John Regan and Joe McCaffrey for helping us with our understanding of the brief and helping us locate required information. We would also like to thank the Maynooth University Theoretical Physics department for providing us with all possible assistance to help us get through this morbid degree.

References

[1] A. D. Goulding, J. E. Greene, D. J. Setton, *et al.*, "UNCOVER: The Growth of the First Massive Black Holes from JWST/NIRSpec-Spectroscopic Redshift Confirmation of an X-Ray Luminous AGN at z = 10.1,", vol. 955, no. 1, L24, p. L24, Sep. 2023. DOI: 10.3847/2041-8213/acf7c5. arXiv: 2308.02750 [astro-ph.GA].

[2] R. L. Larson, S. L. Finkelstein, D. D. Kocevski, *et al.*, "A CEERS Discovery of an Accreting Supermassive Black Hole 570 Myr after the Big Bang: Identifying a Progenitor of Massive z > 6 Quasars,", vol. 953, no. 2, L29, p. L29, Aug. 2023. DOI: 10.3847/2041-8213/ace619. arXiv: 2303.08918 [astro-ph.GA].

[3] R. Maiolino, S. Arribas, A. Bunker, *et al.*, *Confirming Population III or a Direct Collapse Black Hole in the halo of GN-z11 at z=10.6*, JWST Proposal. Cycle 3, ID. #5086, Feb. 2024.

[4] O. E. Kovács, Á. Bogdán, P. Natarajan, *et al.*, "A Candidate Supermassive Black Hole in a Gravitationally Lensed Galaxy at Z ≈ 10,", vol. 965, no. 2, L21, p. L21, Apr. 2024. DOI: 10.3847/2041-8213/ad391f. arXiv: 2403.14745 [astro-ph.GA].

[5] F. Pacucci, P. Natarajan, M. Volonteri, *et al.*, "Conditions for optimal growth of black hole seeds," *The Astrophysical Journal Letters*, vol. 850, no. 2, p. L42, Dec. 2017, ISSN: 2041-8213. DOI: 10.3847/2041-8213/aa9aea. [Online]. Available: http://dx.doi.org/10.3847/2041-8213/aa9aea.

[6] T. Abel, G. L. Bryan, and M. L. Norman, "The formation of the first star in the universe," *Science*, vol. 295, no. 5552, pp. 93–98, Jan. 2002, ISSN: 1095-9203. DOI: 10.1126/science.1063991. [Online]. Available: http://dx.doi.org/10.1126/science.1063991.

[7] M. C. Begelman, M. Volonteri, and M. J. Rees, "Formation of supermassive black holes by direct collapse in pre-galactic haloes,", vol. 370, no. 1, pp. 289–298, Jul. 2006. DOI: 10.1111/j.1365-2966.2006.10467.x. arXiv: astro-ph/0602363 [astro-ph].

[8] H. Bondi, "On spherically symmetrical accretion,", vol. 112, p. 195, Jan. 1952. DOI: 10.1093/mnras/112.2.195.

[9] F. Pacucci, M. Volonteri, and A. Ferrara, "The growth efficiency of high-redshift black holes," *Monthly Notices of the Royal Astronomical Society*, vol. 452, no. 2, pp. 1922–1933, Jul. 2015, ISSN: 0035-8711. DOI: 10.1093/mnras/stv1465. eprint: https://academic.oup.com/mnras/article-pdf/452/2/1922/18508837/stv1465.pdf. [Online]. Available: https://doi.org/10.1093/mnras/stv1465.

[10] M. C. Begelman, "Can a spherically accreting black hole radiate very near the Eddington limit?", vol. 187, pp. 237–251, Apr. 1979. DOI: 10.1093/mnras/187.2.237.

[11] K. Park, M. Ricotti, P. Natarajan, *et al.*, "Bulge-driven fueling of seed black holes," *The Astrophysical Journal*, vol. 818, no. 2, p. 184, Feb. 2016, ISSN: 1538-4357. DOI: 10.3847/0004-637x/818/2/184. [Online]. Available: http://dx.doi.org/10.3847/0004-637X/818/2/184.

[12] K. Inayoshi, Z. Haiman, and J. P. Ostriker, "Hyper-eddington accretion flows on to massive black holes," *Monthly Notices of the Royal Astronomical Society*, vol. 459, no. 4, pp. 3738–3755, Apr. 2016, ISSN: 1365-2966. DOI: 10.1093/mnras/stw836. [Online]. Available: http://dx.doi.org/10.1093/mnras/stw836.

[13] R. Narayan, S. Kato, and F. Honma, "Global structure and dynamics of advection-dominated accretion flows around black holes," *The Astrophysical Journal*, vol. 476, no. 1, pp. 49–60, Feb. 1997, ISSN: 1538-4357. DOI: 10.1086/303591. [Online]. Available: http://dx.doi.org/10.1086/303591.

[14] M. C. Begelman and M. Volonteri, "Hyperaccreting black holes in galactic nuclei," *Monthly Notices of the Royal Astronomical Society*, vol. 464, no. 1, pp. 1102–1107, Sep. 2016, ISSN: 1365-2966. DOI: 10.1093/mnras/stw2446. [Online]. Available: http://dx.doi.org/10.1093/mnras/stw2446.

[15] F. I. Pelupessy, T. Di Matteo, and B. Ciardi, "How Rapidly Do Supermassive Black Hole "Seeds" Grow at Early Times?", vol. 665, no. 1, pp. 107–119, Aug. 2007. DOI: 10.1086/519235. arXiv: astro-ph/0703773 [astro-ph].

[16] M. A. Alvarez, J. H. Wise, and T. Abel, "Accretion onto the First Stellar-Mass Black Holes,", vol. 701, no. 2, pp. L133–L137, Aug. 2009. DOI: 10.1088/0004-637X/701/2/L133. arXiv: 0811.0820 [astro-ph].

[17] A. Ferrara, S. Salvadori, B. Yue, *et al.*, "Initial mass function of intermediate-mass black hole seeds," *Monthly Notices of the Royal Astronomical Society*, vol. 443, no. 3, pp. 2410–2425, Jul. 2014, ISSN: 0035-8711. DOI: 10.1093/mnras/stu1280. [Online]. Available: http://dx.doi.org/10.1093/mnras/stu1280.

[18] S. Hirano, T. Hosokawa, N. Yoshida, *et al.*, "One hundred first stars: Protostellar evolution and the final masses," *The Astrophysical Journal*, vol. 781, no. 2, p. 60, Jan. 2014, ISSN: 1538-4357. DOI: 10.1088/0004-637x/781/2/60. [Online]. Available: http://dx.doi.org/10.1088/0004-637X/781/2/60.

[19] F. Pacucci, A. Loeb, and S. Salvadori, "Gravitational wave sources from Pop III stars are preferentially located within the cores of their host Galaxies," *Monthly Notices of the Royal Astronomical Society: Letters*, vol. 471, no. 1, pp. L72–L76, Jul. 2017, ISSN: 1745-3925. DOI: 10.1093/mnrasl/slx111. eprint: https://academic.oup.com/mnrasl/article-pdf/471/1/L72/56953990/mnrasl_471_1_l72.pdf. [Online]. Available: https://doi.org/10.1093/mnrasl/slx111.

[20] S. E. Woosley, A. Heger, and T. A. Weaver, "The evolution and explosion of massive stars," *Reviews of Modern Physics*, vol. 74, no. 4, pp. 1015–1071, Nov. 2002. DOI: 10.1103/RevModPhys.74.1015.

[21] A. Comastri, R. Gilli, A. Marconi, *et al.*, "Mass without radiation: Heavily obscured agns, the x-ray background, and the black hole mass density," *Astronomy amp; Astrophysics*, vol. 574, p. L10, Feb. 2015, ISSN: 1432-0746. DOI: 10.1051/0004-6361/201425496. [Online]. Available: http://dx.doi.org/10.1051/0004-6361/201425496.

[22] E. Pezzulli, R. Valiante, M. C. Orofino, *et al.*, "Faint progenitors of luminous z 6 quasars: Why do not we see them?" *Monthly Notices of the Royal Astronomical Society*, vol. 466, no. 2, pp. 2131–2142, Dec. 2016, ISSN: 0035-8711. DOI: 10.1093/mnras/stw3243. eprint: https://academic.oup.com/mnras/article-pdf/466/2/2131/10868312/stw3243.pdf. [Online]. Available: https://doi.org/10.1093/mnras/stw3243.

[23] A. Sesana, M. Volonteri, and F. Haardt, "The imprint of massive black hole formation models on the LISA data stream," *Monthly Notices of the Royal Astronomical Society*, vol. 377, no. 4, pp. 1711–1716, May 2007, ISSN: 0035-8711. DOI: 10.1111/j.1365-2966.2007.11734.x. eprint: https://academic.oup.com/mnras/article-pdf/377/4/1711/3812759/mnras0377-1711.pdf. [Online]. Available: https://doi.org/10.1111/j.1365-2966.2007.11734.x.

[24] T. Tanaka and Z. Haiman, "The assembly of supermassive black holes at high redshifts," *The Astrophysical Journal*, vol. 696, no. 2, pp. 1798–1822, Apr. 2009, ISSN: 1538-4357. DOI: 10.1088/0004-637x/696/2/1798. [Online]. Available: http://dx.doi.org/10.1088/0004-637X/696/2/1798.

[25] D. Masters, P. Capak, M. Salvato, *et al.*, "Evolution of the quasar luminosity function over 3 lt;zlt; 5 in the cosmos survey field," *The Astrophysical Journal*, vol. 755, no. 2, p. 169, Aug. 2012, ISSN: 1538-4357. DOI: 10.1088/0004-637x/755/2/169. [Online]. Available: http://dx.doi.org/10.1088/0004-637X/755/2/169.

[26] S. Basu and A. Das, "The mass function of supermassive black holes in the direct-collapse scenario," *The Astrophysical Journal Letters*, vol. 879, no. 1, p. L3, Jun. 2019, ISSN: 2041-8213. DOI: 10.3847/2041-8213/ab2646. [Online]. Available: http://dx.doi.org/10.3847/2041-8213/ab2646.

[27] N. Chen, Y. Ni, M. Tremmel, *et al.*, "Dynamical friction modelling of massive black holes in cosmological simulations and effects on merger rate predictions," *Monthly Notices of the Royal Astronomical Society*, vol. 510, no. 1, pp. 531–550, Nov. 2021, ISSN: 0035-8711. DOI: 10.1093/mnras/stab3411. eprint: https://academic.oup.com/mnras/article-pdf/510/1/531/41833490/stab3411.pdf. [Online]. Available: https://doi.org/10.1093/mnras/stab3411.

```
    '''
    Python code illustrating the optimal conditions for black hole growth and comparing
    our model with actual data from the JWST investigations
    (Figure 1 & 3)
    Author: Conor VanDuyvenvoorde & Aidan Doyle

    '''
#importing packages

import numpy as np
import matplotlib.pyplot as plt
import scipy
from scipy.integrate import quad

N = 600 # number of timesteps

#constants
Omega_0 = 0.3 #current day matter density
```

```
Omega_Lam = 0.7 # cosmological constant
c = 3 * (10 ** 8) #speed of light in a vacuum
G = 6.6743 * (10 ** -11) #gravitaional constant
kappa_T = 5988000 #Thompson opacity, calculation referenced in paper
H_0 = 2.2964 * (10 ** -18) #Hubble constant
C = 24 #(4 * np.pi * G) / (c * kappa_T * H_0)
#actual constant was off by a factor of 10 ** 7 so we used 24 as a close estimate

#defining arrays used for plotting

z = np.linspace(20, 7, N)
integral = np.zeros(N-1)
expn_s = np.zeros(N-1)
expn_l = np.zeros(N-1)
mass_s = np.zeros(N)
mass_l = np.zeros(N)
D_l = np.zeros(N)
Fedd_l = np.zeros(N)
s_scale_cond = np.zeros(10**6)
l_scale_cond = np.zeros(10**6)
Ang_1_cond = np.zeros(10**6)
Ang_2_cond = np.zeros(10**6)
gnd = np.linspace(10 ** (-2), 10 ** 12,10 **6) #gas number density for plotting the conditions

#making N random numbers for the duty cycle and f_edd for the small black hole seed
as they will always be in the ineffecient region
D_s = np.random.uniform(0, 0.5, N)
Fedd_s = np.random.uniform(0, 1, N)

#uniform distributions of size N for the gas number density (the gas number density
changes over time so we just assumed it was drawn from a uniform distribution at each timestep)
gas_numb_dens_s = 10 ** (np.random.uniform(-2, 8, N))
gas_numb_dens_l = 10 ** (np.random.uniform(-2, 8, N))

#initial conditions
mass_s[0] = 10 ** 2
mass_l[0] = 10 ** 5
gas_numb_dens_s[0] = 5 * (10 ** 6)
gas_numb_dens_l[0] = 10 ** 7


def Epsilon(a):
    return ((1+a) * (((((1 + a) ** 2) * ((Omega_0 * a) + 1)) -
    ((Omega_Lam * a * (a + 2)))) ** (1 / 2))) ** (-1)

for i in range(N-1):
    integral[i] = quad(Epsilon, z[i+1], z[i])[0]

    #conditions for efficient black hole growth
    condition_1 = (mass_l[i] >= (10 ** -11) * ((gas_numb_dens_l[i])**2)) #small scale condition
    condition_2 = (mass_l[i] >= (2.2 *(10 ** 13)) * ((gas_numb_dens_l[i]) ** (-5/4)))
    #angular momentum condition with lambda_B_crit used

    if condition_1 and condition_2:
        D_l[i] = np.random.uniform(0.5, 1)
        Fedd_l[i] = np.random.uniform(1, 100)

    else:
```

```
        D_l[i] = np.random.uniform(0, 0.5)
        Fedd_l[i] = np.random.uniform(0, 1)

    expn_l[i] = np.exp(D_l[i] * Fedd_l[i] * C * integral[i])
    expn_s[i] = np.exp(D_s[i] * Fedd_s[i] * C * integral[i])

    mass_l[i+1] = mass_l[i] * expn_l[i]
    mass_s[i+1] = mass_s[i] * expn_s[i]

for i in range(len(s_scale_cond)):
    s_scale_cond[i] = (10**(-11)) * ((gnd[i]) ** 2)
    l_scale_cond[i] = (10 ** 9) * ((gnd[i]) ** (-1))
    Ang_1_cond[i] = (2.2 *(10 ** 19)) * ((gnd[i]) ** (-5/4)) * (10 ** (-6))
    Ang_2_cond[i] = (2.2 *(10 ** 19)) * ((gnd[i]) ** (-5/4)) * (10 ** (-9))

#plot of figure 1(a)
plt.figure('Figure 1(a)',figsize = (8, 6))
plt.title('')
plt.plot(gas_numb_dens_l[0], mass_l[0],marker = 'o', markersize = '10',
markerfacecolor = 'black',markeredgecolor = 'black')
plt.plot(gas_numb_dens_s[0], mass_s[0],marker = 'o', markersize = '10',
markerfacecolor = 'black',markeredgecolor = 'black')
plt.plot(gas_numb_dens_s, mass_s, color = 'grey', alpha = 0.7)
plt.plot(gas_numb_dens_l, mass_l, color = 'grey', linewidth = 0.8, alpha = 0.7)
plt.plot(gnd, s_scale_cond, color = 'r', label = "Small scale condition")
plt.plot(gnd, l_scale_cond, color = 'b', label = "Large scale condition")
plt.plot(gnd, Ang_1_cond, color = 'g', linestyle = '--', label = "Angular momentum (10^-
2)")
plt.plot(gnd, Ang_2_cond, color = 'g', linestyle = ':', label = "Angular momentum (10^-
3)")
plt.tick_params(direction = 'in', right = True, top = True)
plt.yscale('symlog')
plt.xscale('symlog')
plt.xlabel('Gas Number Density [ $cm^{-3}$]', fontsize = '15')
plt.ylabel('Black Hole Mass [$M_{\odot}$]', fontsize = '15')
plt.xlim(10 ** -3, 10 ** 8)
plt.ylim(10, 10 ** 10)
plt.xticks( fontsize = '15')
plt.yticks( fontsize = '15')
plt.fill_between(gnd,s_scale_cond, color = "r", alpha = 0.3)
plt.fill_between(gnd,l_scale_cond, s_scale_cond, color = 'w',alpha = 1 )
plt.fill_between(gnd,s_scale_cond,np.max(s_scale_cond), color = 'g', alpha = 0.3)
plt.fill_between(gnd,Ang_1_cond, s_scale_cond, color = "w", alpha = 1)

#plot of figure 1(b)
plt.figure('Figure 1(b)', figsize = (8, 6))
plt.xscale('log')
plt.yscale('symlog')
plt.tick_params(direction = 'in', right = True, top = True, )
plt.xlabel('Gas Number Density [ $cm^{-3}$]', fontsize = '15')
plt.ylabel('Black Hole Mass [$M_{\odot}$]', fontsize = '15')
plt.xlim(10 ** (4), 10 ** 8)
plt.ylim(10, 10 ** 10)
plt.xticks( fontsize = '14')
plt.yticks( fontsize = '14')
plt.plot(gas_numb_dens_l[0], mass_l[0],marker = 'o', markersize = '5', markerfacecolor = 'green',
markeredgecolor = 'black')
plt.plot(gas_numb_dens_l[0], mass_l[-1],marker = 'o', markersize = '5', markerfacecolor = 'green',
```

```
markeredgecolor = 'black')
plt.plot(gas_numb_dens_s[0], mass_s[0],marker = 'o', markersize = '5', markerfacecolor = 'red',
markeredgecolor = 'black')
plt.plot(gas_numb_dens_s[0], mass_s[-1],marker = 'o', markersize = '5',
markerfacecolor = 'red',markeredgecolor = 'black')
plt.plot([gas_numb_dens_l[0], gas_numb_dens_l[0]], [mass_l[0], mass_l[-1]], color = 'black')
plt.plot([gas_numb_dens_s[0], gas_numb_dens_s[0]], [mass_s[0], mass_s[-1]], color = 'black')
plt.text(1.2 * (10 **7), mass_l[-1], 'z = 7', fontsize = '13')
plt.text(1.2 * (10 **7), mass_l[0], 'z = 20', fontsize = '13')
plt.text(1.1 * gas_numb_dens_s[0], mass_s[-1], 'z = 7', fontsize = '13')
plt.text(1.1 * gas_numb_dens_s[0], 50, 'z = 20', fontsize = '13')

plt.plot(gnd, s_scale_cond, color = 'r', label = "Small scale condition")
plt.plot(gnd, l_scale_cond, color = 'b', label = "Large scale condition")
plt.plot(gnd, Ang_1_cond, color = 'g', linestyle = '--', label =
r"Angular momentum ($\lambda_B = 10^{-2}$)")
plt.plot(gnd, Ang_2_cond, color = 'g', linestyle = ':', label =
r"Angular momentum ($\lambda_B = 10^{-3}$)")
plt.legend(framealpha = 0, loc = 'upper left', fontsize = '15')

plt.fill_between(gnd, s_scale_cond, color = "r", alpha = 0.3)
plt.fill_between(gnd, l_scale_cond, s_scale_cond, color = 'w',alpha = 1 )
plt.fill_between(gnd, s_scale_cond,np.max(s_scale_cond), color = 'g', alpha = 0.3)
plt.fill_between(gnd, Ang_1_cond, s_scale_cond, color = "w", alpha = 1)

#plot of figure 1(c)
plt.figure('Figure 1(c)', figsize = (10, 4.3))
plt.xlabel('Redshift', fontsize = '15')
plt.ylabel(r'Log($M_{\bullet}$)[$M_{\odot}$]', fontsize = '15')
plt.tick_params(direction = 'in', right = True, top = True, )
plt.plot(z, np.log10(mass_l), color = 'green')
plt.plot(z, np.log10(mass_s), color = 'red')
plt.text(14.5, 6.5, 'High-mass Seed', fontsize = '15', color = 'green')
plt.text(13.5, 2.5, 'Low-mass Seed', fontsize = '15', color = 'red')
plt.xlim(20, 6.5)
plt.ylim(1,10)
plt.yticks([1,2,3,4,5,6,7,8,9,10], fontsize = '15')
plt.xticks([20, 18, 16, 14, 12, 10, 8], fontsize = '15')



#plot of figure 3
plt.figure('Figure 3', figsize = (10,4.3))
plt.xlabel('Redshift', fontsize = '15')
plt.ylabel(r'Log($M_{\bullet}$)[$M_{\odot}$]', fontsize = '15')
plt.tick_params(direction = 'in', right = True, top = True, )
plt.plot(z, np.log10(mass_l), color = 'green')
plt.plot(z, np.log10(mass_s), color = 'red')
plt.plot(10.6, np.log10(2 * (10 ** 6)), label = 'GN-Z11',  marker = 'o',
markersize = '12', markerfacecolor = 'purple', markeredgecolor = 'purple')
plt.plot(10.1, np.log10(4 * (10 ** 7)), label = 'UHZ-1',  marker = 'o',
markersize = '12', markerfacecolor = 'red', markeredgecolor = 'red')
plt.plot(10, np.log10(8 * (10 ** 7)), label = 'GHZ-9',  marker = 'o',
markersize = '12', markerfacecolor = 'blue', markeredgecolor = 'blue')
plt.plot(8.7, np.log10(9 * (10 ** 6)), label = 'CEERS-1019',  marker = 'o',
markersize = '12', markerfacecolor = 'orange', markeredgecolor = 'orange')
plt.text(11, 5.65, 'GN-Z11', fontsize = '13', color = 'black')
plt.text(11.3, 7.4, 'UHZ-1', fontsize = '13', color = 'black')
```

```
plt.text(10, 8.3, 'GHZ-9', fontsize = '13', color = 'black')
plt.text(9, 6.3, 'CEERS-1019', fontsize = '13', color = 'black')
plt.legend(loc = 'upper left', fontsize = '15')
plt.xlim(20, 6)
plt.ylim(1,10)
plt.xticks([20, 18, 16, 14, 12, 10, 8], fontsize = '15')
plt.yticks([1,2,3,4,5,6,7,8,9,10], fontsize = '15')
plt.show()


    '''
    Python code illustrating the probabilities of Pop-III and DCBHs that will form
    in the efficient region
    (Figure 2)
    Author: Conor VanDuyvenvoorde & Aidan Doyle

    '''
import numpy as np
import matplotlib.pyplot as plt
import matplotlib.ticker as ticker
from scipy.stats import norm
from scipy.integrate import quad

N = (10 ** 6) - 999 #Number of Pop III black hole seeds given the distribution
a = 6 * (10 ** 5) #Number of Pop III black hole seeds to the right of the
pair instability supernovae gap(100 - 160 solar masses)

#defining arrays used for plotting

mu , sigma = 5.1, 0.2
x_axis = np.linspace(10 ** -4, 10, N)
DCBH_x = 10 ** (np.random.normal(5.1, 0.2, 999))
DCBH_y = 10 ** (np.random.uniform(4, 8, 999))
PopIII_x_axis_1 = np.linspace(1, 2, N-a)
PopIII_x_axis_2 = np.linspace(np.log10(160), 3, a)
PopIII_x_axis = np.hstack((PopIII_x_axis_1,PopIII_x_axis_2))
PopIII_y = 10 ** (np.random.uniform(4, 8, N))
colour = []
count = np.zeros(len(DCBH_x))
s_scale_cond = np.zeros(10**6)
l_scale_cond = np.zeros(10**6)
Ang_1_cond = np.zeros(10**6)
Ang_2_cond = np.zeros(10**6)
gnd = np.linspace(10 ** (-2), 10 ** 12,10 **6)
DCBH_curve = norm.pdf(x_axis, mu, sigma)
PopIII_curve = (2000/ 3) * ((10 **x_axis) ** (-2.35)) * np.exp(-(10/ (10 ** x_axis)))

#setting up conditions for plotting

for i in range(len(s_scale_cond)):
    s_scale_cond[i] = (10**(-11)) * ((gnd[i]) ** 2)
    l_scale_cond[i] = (10 ** 9) * ((gnd[i]) ** (-1))
    Ang_1_cond[i] = (2.2 *(10 ** 19)) * ((gnd[i]) ** (-5/4)) * (10 ** (-6))
    Ang_2_cond[i] = (2.2 *(10 ** 19)) * ((gnd[i]) ** (-5/4)) * (10 ** (-9))

#showing which points are in the efficient region by making them green
for i in range(len(DCBH_x)):

    condition_1 = (DCBH_x[i] >= (10 ** -11) * ((DCBH_y[i]) ** 2 ))
```

```
    condition_2 = (DCBH_x[i] >= (2.2 *(10 ** 13)) * ((DCBH_y[i]) ** (-5/4)))

    if condition_1 and condition_2:
        colour.append('green')
        count[i] = True
    else:
        colour.append('black')
        count[i] = False

print("Number of black holes formed in the efficient region =", (np.count_nonzero(count)))
#printing the number of black holes in the efficient region

#defining the IMF of the Pop-III black holes given in report
def custompdf(x):
    return (2000/ 3) * ((10 **x) ** (-2.35)) * np.exp(-(10/ (10 ** x)))

#trapazoidal rule to get cdf
cdf_values = np.cumsum(custompdf(PopIII_x_axis)) * (PopIII_x_axis[1] - PopIII_x_axis[0])

#normalise the cdf to [0, 1]
cdf_values /= cdf_values[-1]

uniform_samples = np.random.random(N)

#interpolate to get custom random variables from the given distribution
customsamples = np.interp(uniform_samples, cdf_values, PopIII_x_axis)

#Plot of Figure 2
plt.figure('Figure 2', figsize = (8,6))
plt.plot(s_scale_cond, gnd, color = 'r', label = "Small scale")
plt.plot(l_scale_cond, gnd, color = 'b', label = "Large scale")
plt.plot(Ang_1_cond, gnd, color = 'g', label = "Angular momentum")
plt.fill_betweenx(gnd, np.max(s_scale_cond), s_scale_cond, color = 'g', alpha = 0.2)
plt.fill_betweenx(gnd, Ang_1_cond, s_scale_cond, color = 'white', alpha = 1)
plt.legend(loc = 'lower right', framealpha = 0)
plt.tick_params(direction = 'in', left = True, top = True, length = 8)
plt.xlabel('Black Hole Mass [$M_{\odot}$]', fontsize = '13')
plt.ylabel('Gas Number Density [ $cm^{-3}$]', fontsize = '13')
plt.xscale('symlog')
plt.yscale('log')
plt.xticks(fontsize = '13')
plt.yticks(fontsize = '13')
plt.xlim(1, 10 ** 10)
plt.ylim(10 ** 4, 10 ** 8)
plt.text(10 ** 6, 10 ** 7, 'Accretion is very efficient \n   in this region', fontsize = '12')
plt.text(5 * (10 ** 5),5 * (10 ** 5), 'DCBH', color = 'orange', fontsize = '13')
plt.text(40, 5 * (10 ** 5), 'Pop III', color = 'orange', fontsize = '13')

#scatter plots of the black holes making the ones in the efficient region green
plt.scatter(10 ** customsamples, PopIII_y, s = 0.5, color = 'black')
for i in range(999):
    plt.scatter(DCBH_x[i], DCBH_y[i], s = 0.5, c = colour[i])

#plots of the IMFs against the right axis
plt.twinx()
plt.tick_params(direction = 'in', left = True, top = True, length = 2, width = 0.5)
plt.plot(10 ** x_axis,DCBH_curve/2, c = 'orange')
plt.plot(10 ** x_axis,PopIII_curve, c = 'orange')
```

```
plt.ylabel('IMF Probability', fontsize = '13')
plt.xticks(fontsize = '13')
plt.yticks(fontsize = '13')
plt.xlim(10, 10 ** 10)
plt.ylim(0, 1)
plt.show()
```